THE JOURNAL OF PHYSICAL CHEMISTRY C

Article

pubs.acs.org/JPCC

The First Halide-Free Bimetallic Aluminum Borohydride: Synthesis, Structure, Stability, and Decomposition Pathway

Iurii Dovgaliuk,[†] Voraksmy Ban,[†] Yolanda Sadikin,[‡] Radovan Černý,[‡] Lionel Aranda,[§] Nicola Casati,[∥] Michel Devillers,[†] and Yaroslav Filinchuk*[,†]

[†]Institute of Condensed Matter and Nanosciences, Université catholique de Louvain, Place L. Pasteur 1, 1348 Louvain-la-Neuve, Belgium

[‡]Laboratory of Crystallography, DPMC-MaNEP, University of Geneva, quai Ernest-Ansermet 24, 1211 Geneva, Switzerland

[§]Faculté des Sciences, Institut Jean Lamour (UMR 7198), BP 70239, 54506 Vandoeuvre-lès-Nancy, France

[∥]Swiss Light Source, Paul Scherrer Institute, WLGA/229, 5232 Villigen, Switzerland

Supporting Information

ABSTRACT: Interaction of solid KBH_4 with liquid $Al(BH_4)_3$ at room temperature yields a solid bimetallic borohydride $KAl(BH_4)_4$. According to the synchrotron X-ray powder diffraction, its crystal structure (space group *Fddd*, a = 9.7405(3), b = 12.4500(4), and c = 14.6975(4) Å) contains a substantially distorted tetrahedral $[Al(BH_4)_4]^-$ anion, where the borohydride groups are coordinated to aluminum atoms via edges. The η^2-coordination of BH_4^- is confirmed by the infrared and Raman spectroscopies. The title compound is the first aluminum-based borohydride complex not stabilized by halide anions or by bulky organic cations. It is not isostructural to bimetallic chlorides, where more regular tetrahedral $AlCl_4^-$ anions are present. Instead, it is isomorphic to the LT phase of $TbAsO_4$ and can be also viewed as consisting of two interpenetrated *dia*-type nets where BH_4 ligand is bridging Al and K cations. Variable temperature X-ray powder diffraction, TGA, DSC, and TGA-MS data reveal a single step of decomposition at 160 °C, with an evolution of hydrogen and some amount of diborane. Aluminum borohydride is not released in significant amounts; however, some crystalline KBH_4 forms upon decomposition. The higher decomposition temperature than in chloride-substituted Li−Al (70 °C) and Na−Al (90 °C) borohydrides suggests that the larger alkali metal cations (weaker Pearson acids) stabilize the weak Pearson base, $[Al(BH_4)_4]^-$.

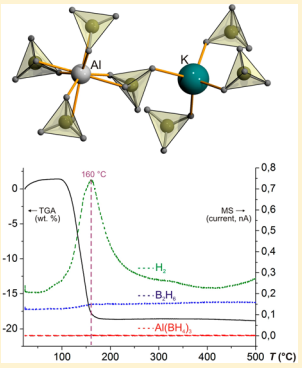

INTRODUCTION

During the recent years, metal borohydride complexes and their derivatives are among the most exciting materials for potential hydrogen storage due to their high hydrogen content.[1] Regarding the hydrogen gravimetric and volumetric system targets, recently revised by the U.S. Department of Energy to 5.5 wt % and 40 g/L,[2] most of the alkali and alkali-earth metal borohydrides match them. However, metal borohydrides are quite stable for hydrogen release by thermolysis as they decompose at high temperatures (about 470 °C for $LiBH_4$ and 290−500 °C for $Mg(BH_4)_2$).[3,4] The temperature of desorption can be dramatically reduced for bimetallic borohydride complexes, where the decomposition temperature decreases with increasing Pauling electronegativity for complex anions.[5,6] The increasing covalence in M−H bonding weakens the B−H bonding and improves thermal decomposition properties of bimetallic complexes. Among the so far published bimetallic complex borohydrides, there are several that match the temperature range of 60−120 °C applicable for fuel cells:[7] "$Li_4Al_3(BH_4)_{13}$" containing some chloride on a borohydride site,[8] $Na[Al(BH_4)_{4-x}Cl_x]$,[9] $NaZn_2(BH_4)_5$, $NaZn(BH_4)_3$,[10] $KCd(BH_4)_3$, $K_2Cd(BH_4)_4$.[11] All the mentioned bimetallic borohydrides evolve diborane (B_2H_6) as hydrogen desorption byproduct which prevents full reversibility and is undesirable for fuel cell applications. This disadvantage is absent for borohydrides which decompose at higher temperatures,[12] in particular for the bimetallic series (Li, Na, K)[(Sc, Y)-$(BH_4)_4$].[13−16] Because of the widely used mechanochemical synthesis of novel borohydrides starting from metal borohydrides and halides, most bimetallic systems contain metal halides as secondary phases as well as halide substitution on the borohydride sites.[17,18] Besides stabilizing new phases that may not exist in Cl-free systems,[19] this considerably decreases gravimetric capacities of the novel hydrides. From this point of view, it is important to carry out synthesis of new borohydrides by addition with other complex forming borohydrides, like $Al(BH_4)_3$.[20]

Herein we report on the synthesis, crystal structure, and Raman vibrational spectra together with thermal analysis of $K[Al(BH_4)_4]$ which was first obtained by Semenenko et al.[21] The synthesis was performed with liquid $Al(BH_4)_3$ and KBH_4 with the aim to prevent formation of possible halide-containing

Received: September 15, 2013
Revised: December 16, 2013
Published: December 16, 2013

phases, common in case of metathesis reactions between borohydrides and halides. The crystal structure was determined by synchrotron powder diffraction, and further structural characterization was performed with Raman and IR spectroscopy. The thermal stability of the title compound up to 160 °C is considerably higher than 70 and 90 °C for the related $Li_4Al_3(BH_4)_{13}$ and $Na[Al(BH_4)_{4-x}Cl_x]$.[8,9] Unlike the Li-based phase, the title compound does not desorb $Al(BH_4)_3$; however, it eliminates diborane as a decomposition byproduct with 20.8 wt % mass loss at 12.7 wt % theoretical hydrogen content.

EXPERIMENTAL DETAILS

Synthesis. *Caution! $Al(BH_4)_3$ is highly pyrophoric and explosive in contact with moisture and air.* In order to prevent explosive reaction of $Al(BH_4)_3$ with air, all manipulations were carried out in nitrogen-filled Plexiglas glovebox. The starting materials are $AlCl_3$ (95% Sigma-Aldrich), KBH_4 (99% Sigma-Aldrich), and $LiBH_4$ (95% Sigma-Aldrich and 96% Boss Chemical Industry Co.). The first stage of the synthesis is the preparation of $Al(BH_4)_3$ from $AlCl_3$ and $LiBH_4$ according to the reaction

$$AlCl_3 + 3LiBH_4 \rightarrow Al(BH_4)_3 + 3LiCl \quad (1)$$

We have developed a modified procedure of those described in refs 20 and 22. The grinded mixture with 5% excess of $LiBH_4$ (Boss Chemical Industry Co.) relative to stoichiometry was steadily heated in the glass flask, connected to a tandem of two liquid nitrogen traps. $Al(BH_4)_3$ starts to evolve as the mixture melts at about 100 °C. At this moment the system was pumped down to 10^{-2} mbar, and the product with some $AlCl_3$ impurity is condensed in the traps. The pumping was ended when the mixture stopped boiling. The content of the first trap was unfrozen and purified by distillation at ambient pressure, all in the nitrogen-filled glovebox. The distillation was carried out with Teflon-coated greaseless ground glass joints using a water cooled Liebig condenser. Only the fraction boiling at 44.5 °C or slightly below was collected in order to separate $Al(BH_4)_3$ from chloride-containing derivatives.

In the second stage of synthesis, 1−2 mL of the fresh $Al(BH_4)_3$ was transferred via a syringe to a bottle with 200 mg of grinded KBH_4 powder with continuous stirring. Reaction 2 took place over 4−6 days:[21]

$$Al(BH_4)_3 + KBH_4 \rightarrow K[Al(BH_4)_4] \quad (2)$$

The excess of volatile $Al(BH_4)_3$ was removed by pumping with an oil pump for a few minutes. The final products of the reaction were identified by X-ray powder diffraction (XRD). After the first soaking of KBH_4 in $Al(BH_4)_3$, the resulting $KAl(BH_4)_4$:KBH_4 weight ratio is about 1:1. It increases successively after the following soakings, i.e. grinding and stirring with $Al(BH_4)_3$ liquid, as observed by Semenenko et al.[21] (Figure S1). Because of the dangerous flammability of $Al(BH_4)_3$, we did not perform the synthesis with liquid−solid ball-milling. It is worth noting that the yield of $K[Al(BH_4)_4]$ considerably depends on the purity of $Al(BH_4)_3$: the monoclinic $KAlCl_4$[23] forms as a side product if $Al(BH_4)_3$ is not purified by distillation (see Figure S2).

A similar procedure was made by soaking the $2LiBH_4$:KBH_4 mixture in excess $Al(BH_4)_3$ and removing its excess in vacuum, yielding $LiK(BH_4)_2$ and $K[Al(BH_4)_4]$ (see Figure S3). The mixtures were grinded with agate mortar in an argon-filled inert glovebox and introduced into 0.7 mm diameter glass capillaries which were sealed with inert vacuum grease for the following powder diffraction and Raman spectroscopic measurements.

Ball-milling of the $9LiBH_4 + 3KBH_4 + 2AlCl_3$ mixture also leads to a formation of $K[Al(BH_4)_4]$, in a mixture with LiCl and $LiK(BH_4)_2$ (see Figure S4). We will not focus our attention on this sample, as it is not Cl-free.

X-ray Powder Diffraction Analysis. Samples were filled into 0.5 mm thin-walled glass capillaries and sealed under an inert atmosphere. Laboratory diffraction data were obtained with a MAR345 diffractometer, rotating anode Mo$K\alpha$ radiation, and XENOCS focusing mirror.

The $2LiBH_4$:KBH_4:$Al(BH_4)_3$ sample was characterized by temperature-variable *in situ* powder X-ray diffraction at SNBL, ESRF (Grenoble, France) with a PILATUS 2M pixel detector and λ = 0.827 27 Å wavelength synchrotron X-ray radiation. Temperature was increased linearly in time using Oxford Cryostream 700+ at 5 °C/min rate. A sample with ∼90 wt % of $KAl(BH_4)_4$ was measured with λ = 0.682 525 Å at room temperature. The 2D images were azimuthally integrated using Fit2D program and data on a LaB_6 standard.[24]

The KBH_4:$Al(BH_4)_3$ sample was studied at Materials Science Beamline at PSI (Villigen Switzerland),[25] using a Mythen II detector and λ = 0.818 109 Å. Temperature was increased from 30 to 210 °C in steps of 10 °C. The $LiBH_4$:KBH_4:$AlCl_3$ sample was measured at room temperature with λ = 0.827 12 Å.

The rehydrogenation of the $K[Al(BH_4)_4]$/KBH_4 sample was tested using a sapphire-based cell for *in situ* synchrotron powder diffraction[26] at Materials Science Beamline, using Mythen II detector and λ = 0.775 045 Å. The starting powder was held in a single-crystal sapphire (Al_2O_3) capillary with 1.09 mm outer diameter. The decomposition of the $K[Al(BH_4)_4]$ under 1 bar of H_2 was performed by heating the capillary from room temperature to 210 °C with 5 °C/min heating rate. The decomposed sample was cooled to 50 °C under 100 bar of H_2; the powder diffraction data were collected on the system for 70 min. An additional experiment was done by heating the same sample to 320 °C and subsequent cooling it from this temperature at 10 °C/min rate to the room temperature under 100 bar of H_2.

The orthorhombic crystal lattice of $K[Al(BH_4)_4]$ was indexed and the structure was solved in *Fddd* space group with the program FOX[27] and refined with the Rietveld method using Fullprof.[28] The symmetry was confirmed with the ADDSYM routine in the program PLATON.[29] The structure was solved and refined with BH_4^- groups as semirigid ideal tetrahedra with one common refined B−H distance of 1.13 Å. No other restraints were used. Rietveld refinement suggested a negligibly small chloride substitution of 0.03(1) on the borohydride site, confirming the Cl-free composition.

Infrared and Raman Spectra. These spectra were recorded at room temperature respectively with a FTIR-8400S Shimadzu spectrophotometer in the 400−4000 cm^{-1} range and with a Bruker RFS 100/s FT-Raman spectrometer (I = 200 mW) in 100−4000 cm^{-1} using a diode-pumped, air-cooled Nd:YAG laser for 1064 nm excitation. For the IR measurements the sample was mixed with KBr matrix in an inert atmosphere. Pure KBr was used for background subtraction.

TGA and DSC Analysis. This analysis was made on powder samples after preliminary X-ray powder diffraction analysis. The data were collected independently with a TGA/SDTA 851 Mettler and a DSC 821 Mettler instrument with the heating rate of 5 °C/min from 25 to 500 °C. The samples for the TGA

dx.doi.org/10.1021/jp409217x | J. Phys. Chem. C 2014, 118, 145−153

and DSC analysis were loaded in the argon inert glovebox into crucibles with caps or sealed into aluminum pans, respectively. The experiments were done under 10 mL/min nitrogen flow to prevent the oxidizing reactions.

TGA Coupled with Mass Spectrometry (MS). TGA-MS was measured using two independent setups: (1) ThermoStar GSD 301T spectrometer coupled with simultaneous TGA/DTA 851 Mettler and (2) Omnistar GSD 301C-Pfeiffer Vacuum spectrometer coupled with SETARAM Setsys Ev 1750 TGA instrument. The measurements were done under 10 mL/min argon flow with the heating rate of 2 °C/min in 25–300 and 20–500 °C temperature ranges, respectively.

RESULTS AND DISCUSSION

Phase Analysis of *in Situ* Synchrotron Powder Diffraction Data. The X-ray powder diffraction analysis was performed for ternary Li–K–Al and binary K–Al borohydride systems; the details are given in the Supporting Information, Figure S3. The trimetallic Li–K–Al–BH_4 system contains $LiBH_4$ as LT and HT polymorphs (within their stability ranges),[30] KBH_4,[31] $LiK(BH_4)_2$,[32] and a new bimetallic phase, $K[Al(BH_4)_4]$. The formation of $K[Al(BH_4)_4]$ is more favorable than that of $Li_4Al_3(BH_4)_{13}$ or a hypothetical $Li[Al(BH_4)_4]$ because the Li atom is a weaker donor of electrons compared to K. In other words, K stabilizes better the $[Al(BH_4)_4]^-$ complex.

The known bimetallic $LiK(BH_4)_2$ forms readily at room temperature, in contrast to the 120 °C annealing required for the $LiBH_4$:KBH_4 sample.[32] Formation of $LiK(BH_4)_2$ in the mild conditions is thus mediated by $Al(BH_4)_3$. It can be explained by partial solubility of solid $LiBH_4$ and KBH_4 borohydrides in liquid $Al(BH_4)_3$, facilitating the addition reaction. Notably, $LiK(BH_4)_2$ in our sample decomposes into the $LiBH_4$ + KBH_4 mixture at much lower temperatures than reported previously, namely at 95 °C against 240 °C attributed to melting and 380 °C for the decomposition.[32] The disappearance of diffraction peaks from $LiK(BH_4)_2$ correlates nicely with increasing intensities from $LiBH_4$ and KBH_4. This observation confirms the theoretical conjecture that $LiK(BH_4)_2$ is unstable with respect to decomposition into $LiBH_4$ and KBH_4,[33] as the decomposition temperatures apparently do not reflect the equilibrium state but the kinetic barriers intrinsic to a particular multicomponent system, in particular by the presence of the Al-based complex, $K[Al(BH_4)_4]$.

We focused our attention on the new bimetallic compound, which we first observed by diffraction in this ternary system. Our further attempts were to obtain and characterize this complex from the binary KBH_4 + $Al(BH_4)_3$ mixture. Two cycles of soaking in excess of $Al(BH_4)_3$ and its removal in vacuum resulted in samples containing ~70 wt % of $K[Al(BH_4)_4]$ with 30% of the remaining KBH_4. The yield can be increased to 90% by a third soaking–vacuum pumping cycle. The important intermediate step in the synthesis is grinding the sample before adding a new portion of $Al(BH_4)_3$. The sample containing 90.1(5) wt % of $K[Al(BH_4)_4]$ was refined by Rietveld method (see Figure 1a).

In situ synchrotron XRD in the 30–210 °C temperature range reveals the decomposition of $K[Al(BH_4)_4]$ at ~180 °C, with an onset at 150–160 °C, into amorphous products and KBH_4. Remarkably, the diffraction intensities of the crystalline KBH_4 are increasing during the decomposition of $K[Al(BH_4)_4]$ (Figure 1b), showing the maximum at 160 °C (Figure S5). This observation complements nicely the thermal analysis and mass spectrometric data, helping to suggest a decomposition reaction pathway (see below).

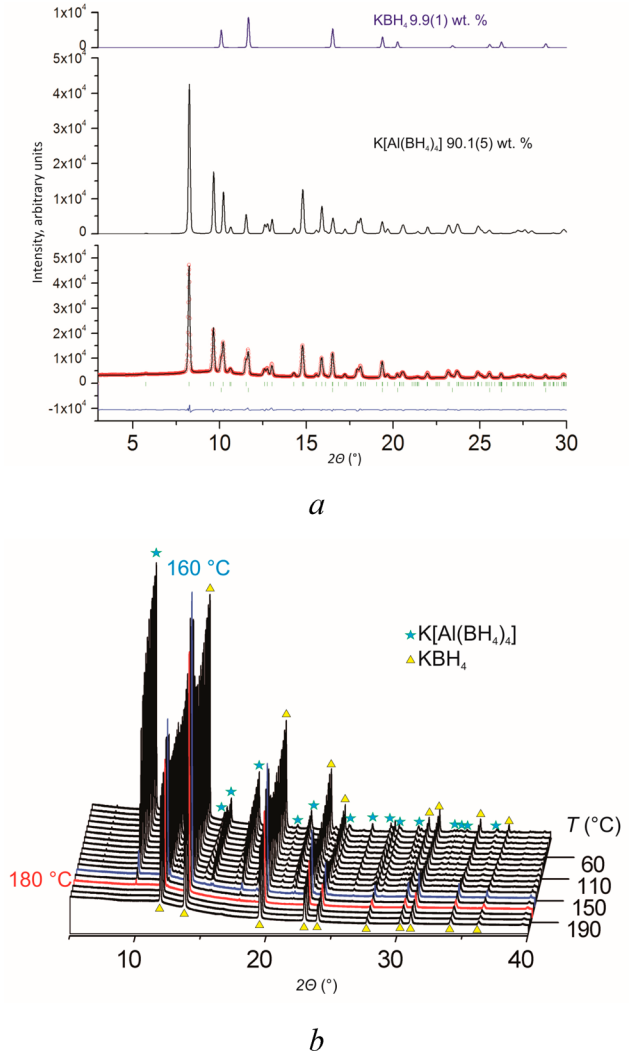

Figure 1. (a) Low-angle part of the Rietveld refinement profile (extending up to 62° in 2θ) for the ESRF synchrotron data, λ = 0.682 525 Å, R_{wp} = 7.55%. $K[Al(BH_4)_4]$: space group *Fddd*, a = 9.7405(3), b = 12.4500(4), and c = 14.6975(4) Å, R_F = 3.8%; KBH_4: *Fm*-3*m*, a = 6.72556(1) Å, R_F = 3.2%. (b) Temperature evolution of powder diffraction patterns for $K[Al(BH_4)_4]$/KBH_4 mixture from 30 to 210 °C, λ = 0.815 60 Å, SLS. Red line highlights the pattern collected right after the decomposition of $K[Al(BH_4)_4]$ at 180 °C, showing Bragg peaks of KBH_4 alone. The blue line shows the maximum intensity of KBH_4 at 160 °C.

Crystal Structure of $K[Al(BH_4)_4]$. The title compound is the first halide-free bimetallic borohydride containing $[Al(BH_4)_4]^-$. The other bimetallic Al-based complexes, such as "$Li_4Al_3(BH_4)_{13}$"[8] and $Na[Al(BH_4)_{4-x}Cl_x]$,[9] are stabilized by Cl-substitution on the borohydride sites, as determined by structural refinements. The only Cl-free complex aluminum borohydride, $[Ph_3MeP][Al(BH_4)_4]$, contains a bulky organic cation,[34] making it inappropriate for hydrogen storage applications. Interestingly, a synthesis involving $AlCl_3$ results in the $K[Al(BH_4)_4]$ phase with cell parameters very similar to those of the chlorine-free compound, indicating low or no substitution of Cl on the BH_4 sites (see Supporting Information).

dx.doi.org/10.1021/jp409217x | J. Phys. Chem. C 2014, 118, 145–153

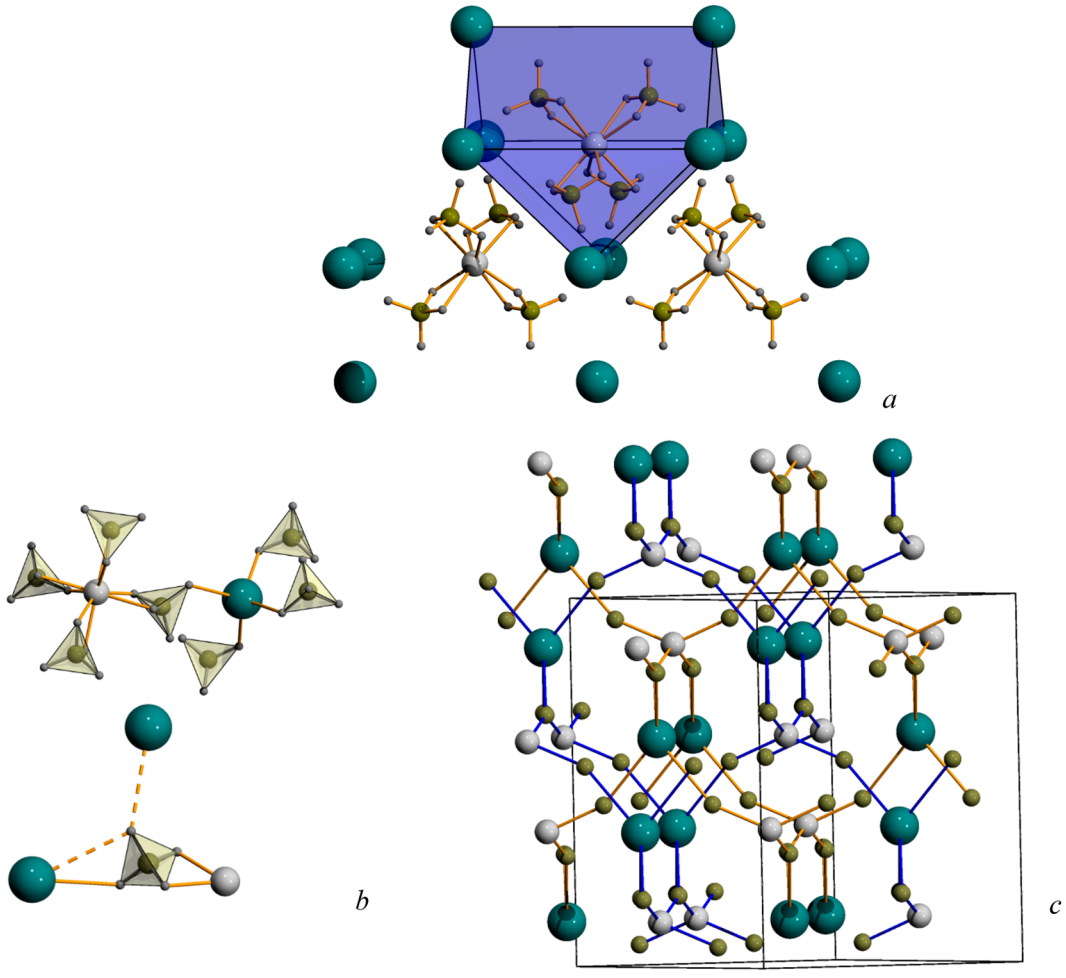

Figure 2. Representations of the crystal structure of $K[Al(BH_4)_4]$. (a) Complex anion $[Al(BH_4)_4]^-$ located in the bicapped trigonal prismatic cage K_8. (b) Coordination environment of K, Al atoms, and the BH_4 group; the dashed lines depict elongated K···H distances completing the coordination for K to 4H + 8H. (c) Two interpenetrated *dia*-type nets; hydrogen atoms are omitted for clarity.

$K[Al(BH_4)_4]$ crystallizes in the orthorhombic space group *Fddd*, as the LT-$TbAsO_4$ prototype,[35] with BH_4^- anions in place of oxygen atoms. The LT phase of $TbAsO_4$ (stable below 27.7 K) is an orthorhombic deformation of the tetragonal HT phase ($I4_1/amd$, $ZrSiO_4$ type) caused by the Jahn–Teller effect. The orthorhombic structure of $K[Al(BH_4)_4]$, stable until its decomposition, is far from a tetragonal prototype. This is certainly due to much stronger deformation of $[Al(BH_4)_4]^-$ from an ideal tetrahedron (see below) as compared to $[AsO_4]^{3-}$.

Metal cations have distorted tetrahedral environments formed by the BH_4^- groups. Aluminum atoms are coordinated to four anions via the BH_2 edges: Al–H1 1.79(1) Å and Al–H3 1.96(1) Å, forming distorted tetrahedral $[Al(BH_4)_4]$ complexes with B–Al–B angles ranging from 97.6(1)° to 135.4(1)°, very close to 100.0(1)°–130.8(2)° in $Li_4Al_3(BH_4)_{13}$.[8] K^+ coordinates the anion asymmetrically via an edge: K–H2 2.55(1) Å, K–H4 3.20(1) Å. The BH_4^- group is coordinated through the vertex to another potassium cation (K–H4 2.92(9) Å), forming T-shaped coordination for the anion and 4 + 4 coordination polyhedron for K with respect to the BH_4^- groups. Disregarding the more distant potassium atom, the borohydride group acts like a nearly linear bridging ligand with Al···B···K angle of 152.7(2)°, similar to Mg···B···Mg angles in $Mg(BH_4)_2$ framework structures.[36,37]

The Al–B distance of 2.262(4) Å is slightly longer than 2.10–2.15 Å in α,β-$Al(BH_4)_3$ where Al coordinates three borohydrides[38,39] and falls in the 2.22–2.35 Å range for the tetracoordinated Al in $Al_3Li_4(BH_4)_{13}$, $[Ph_3MeP][Al(BH_4)_4]$, and $Na[Al(BH_4,Cl)_4]$.[8,9,34] Because of the smaller size of Al^{3+}, the Al–B distances are slightly shorter than 2.27–2.38 Å Sc–B and Y–B bond distances in $K[Sc(BH_4)_4]$ and $K[Y(BH_4)_4]$.[15,16] Remarkably, Y^{3+} and Sc^{3+} coordinate the BH_4 groups via the tetrahedral faces, showing higher coordination numbers and longer metal–hydrogen distances. The short K–B distance of 3.285(4) Å in $K[Al(BH_4)_4]$ (CN = 4 + 4) is similar to the 3.26(1) Å distance in $K[Y(BH_4)_4]$ (CN = 6)[16] and slightly shorter than 3.364 Å in the cubic KBH_4 (CN = 6)[31] or shorter than the short distance of 3.51(4) Å for CN = 8 in $K[Sc(BH_4)_4]$.[15] The longer K–B distance of 3.809(4) Å is comparable to the longest K–B distance of 3.95(2) Å[15] for CN = 8 in $K[Sc(BH_4)_4]$. On the other hand, K^+ with CN = 7 in $LiK(BH_4)_2$ shows more regular K–B distances, falling within 3.40–3.47 Å.[32]

$K[Al(BH_4)_4]$ is not isomorphic to $KAlCl_4$ and $NaAlCl_4$, where much more regular tetrahedral $AlCl_4^-$ anions are present, as well as different coordination polyhedra for alkali metal atoms are observed.[23,40] The title structure can be seen as an ionocovalent compound containing complex anion $[Al(BH_4)_4]^-$ located in the bicapped trigonal prismatic cage K_8

dx.doi.org/10.1021/jp409217x | *J. Phys. Chem. C* 2014, 118, 145–153

(Figure 2a). In the related compound, $Na[Al(BH_4)_{4-x}Cl_x]$,[9] the complex anion is also located in a deformed square prismatic Na_8 cage. The ratio of the average K−B to Al−B distances of 1.57 is quite large (for comparison with other members see Table 3 in ref 41), indicating an important degree of isolation of the complex anion $[Al(BH_4)_4]^-$ in the K_8 cage.

Neglecting four longer K−B distances, the structure of $K[Al(BH_4)_4]$ can be also viewed as a framework formed by two diamond nets (or ZnS nets, considering the K and Al ordering), shown in Figure 2c. The two interpenetrated *dia*-nets are touching each other via one of the two elongated H···K 3.20(1) Å (B···K 3.809(4) Å), shown by the dashed line in Figure 2b. The same topology was found for another complex hydride, $LiZn_2(BH_4)_5$.[10] Double interpenetrated frameworks are much more clearly observed in the absence of complex anions, i.e., in the high-pressure δ-$Mg(BH_4)_2$[37] and two closely related $Cd(BH_4)_2$ polymorphs.[11] The topologies typical for coordination frameworks highlight the role of the borohydride anion acting as the bridging directional ligand.[42]

Infrared and Raman Spectroscopy. The strongest bands in the 2100−2600 cm^{-1} range (Figure 3) correspond to B−H

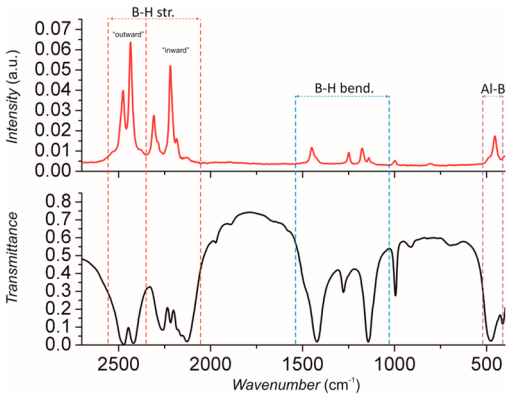

Figure 3. Raman and infrared spectra of $K[Al(BH_4)_4]/KBH_4$ mixture (90.1/9.9 wt %) at room temperature.

stretching, and less intense peaks from 990 to 1300 cm^{-1} can be attributed to B−H bending modes. Only the strongest peak of KBH_4 at 2308 cm^{-1} [43] can be recognized in stretching mode region in the Raman spectrum, the remaining peaks overlap with B−H stretching modes from $K[Al(BH_4)_4]$: the difference of intensities in spectra for different $K[Al(BH_4)_4]/KBH_4$ ratios is shown in the Supporting Information (Figure S4). The other two peaks at 2436 and 2476 cm^{-1} from Raman and 2419 and 2472 cm^{-1} from IR are related to the outward B−H stretching modes from $[Al(BH_4)_4]^-$ with respect to the observed in crystal structure bidentate coordination. The mentioned doublet in the 2400−2600 cm^{-1} range with 50−80 cm^{-1} splitting is typical for bidentately bridged borohydrides.[44,45] Similar peaks were seen at 2440 and 2480 cm^{-1} for $Al_3Li_4(BH_4)_{13}$ in Raman and at 2420 with 2480 cm^{-1} in the infrared spectrum as well as 2444 and 2503 cm^{-1} for $Na[Al(BH_4Cl)_4]$ in Raman spectra.[8,9]

In the region of B−H bending modes, a band at 1249 cm^{-1} corresponds to KBH_4.[34,43] The other peaks at 999, 1140, 1177, and 1450 cm^{-1} in Raman spectrum and 996, 1144, 1278, 1422 cm^{-1} in the IR can be assigned to the BH_2 bending modes in $[Al(BH_4)_4]^-$, similar to $Al_3Li_4(BH_4)_{13}$ complex (near 1000, 1020, 1170, and 1450 cm^{-1} in the Raman spectrum[8]). The sharp bands at 455 and 477 cm^{-1} in both spectra likely correspond to the Al−B stretching mode, also previously seen at 490 cm^{-1} for Li−Al and Na−Al complex borohydrides, as well as for the pure $Al(BH_4)_3$.[8,9,46]

Thermal and Mass Spectrometry Analysis. The TGA and DSC curves of the $K[Al(BH_4)_4]/KBH_4$ (73.1/26.9 wt % from XRD) mixture are shown in Figure 4. Only one sharp

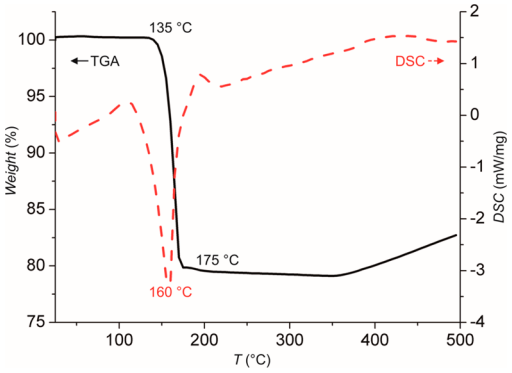

Figure 4. Thermal analysis of $K[Al(BH_4)_4]/KBH_4$ mixture.

endothermic peak with the maximum at 160 °C was detected by DSC analysis in the 25−500 °C temperature range. According to the thermogravimetric analysis and *in situ* XRD, a decomposition of $K[Al(BH_4)_4]$ complex starts at 135 °C and finishes at 175 °C (near 180 °C from XRD). This decomposition profile is significantly different from the previously reported decomposition of presumably pure $K[Al(BH_4)_4]$ by Semenenko et al.,[21] where two endothermic peaks were detected at 132 and 240 °C. According to ref 21, the evolution of diborane and hydrogen was also accompanied by considerable amounts of $Al(BH_4)_3$ desorbing at 130 °C. The total mass loses of 20.8 wt % on our sample is equivalent to 28.5 wt % with respect to the pure $K[Al(BH_4)_4]$. Desorption of $Al(BH_4)_3$ would lead to a much larger weight loss of 56.9 wt % for the pure $K[Al(BH_4)_4]$ or 41.8 wt % for our $K[Al(BH_4)_4]/KBH_4$ (73.1/26.9 wt %) sample. According to our diffraction data, the intensity of KBH_4 peaks increases upon the decomposition of $K[Al(BH_4)_4]$ (Figure S5), providing ∼0.6 mol of KBH_4 upon decomposition of 1 mol of $K[Al(BH_4)_4]$. Taking together with the TGA data, all the observations can be described by the following hypothetic decomposition reaction 3:

$$2K[Al(BH_4)_4] \rightarrow KBH_4 + \text{amorphous } \text{“}KAl_2B_3\text{”} + 2B_2H_6 + 8H_2 \quad (3)$$

This reaction gives 28.5 wt % loss of mass, as observed by the TGA. The absence of diffraction peaks in the decomposed products rules out the formation of the anticipated crystalline phases, such as AlB_2, K−B borides, and KH.

We additionally performed two independent mass spectrometry measurements on the evolving gas products, combined with the simultaneous TGA. Atomic mass units 26 and 27 corresponding to B_2H_6 and 42, 43, 56, 57 and 70−73 amu corresponding to $Al(BH_4)_3$, as observed in decomposition of $Al_3Li_4(BH_4)_{13}$,[51] were chosen as characteristic fragments. From our data shown in Figure 5, diborane release is clearly observed at 160 °C, fully consistent with the maximum of the endothermic peak seen in DSC and weight losses in TGA and TGA-MS data in Figure 6. Due to the fact that 28 *m*/*z* signal in the diborane reference data amounts only to

dx.doi.org/10.1021/jp409217x | J. Phys. Chem. C 2014, 118, 145−153

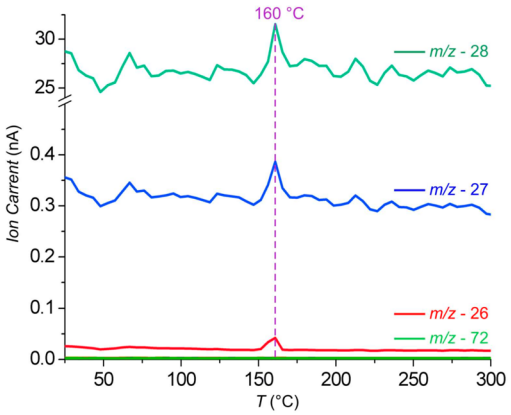

Figure 5. MS curve of evolving gases measured in 25−300 °C temperature range. The lines close to the zero level show the absence of $Al(BH_4)_3$ fragments.

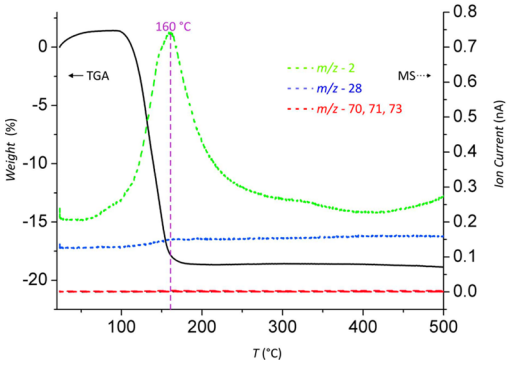

Figure 6. TGA-MS curves in 20−500 °C temperature range for $K[Al(BH_4)_4]/KBH_4$ (85/15 wt %) sample. The current for diborane is considerably lower than for hydrogen. The beam current is practically zero for aluminum borohydride.

~0.5%,[47,48] the likely origin of this peak at the decomposition is the release of molecular nitrogen, which was trapped during the synthesis. The evolution of AlH^+ with 28 m/z as byproduct is also not feasible because this peak has a much smaller abundance (~22%) compared to 27 m/z for Al, as seen for aluminum hydride (alane) decomposition from hydrogen-covered aluminum single crystal surfaces.[49] At the same time, diborane was observed by IR data from decomposition of $Al_3Li_4(BH_4)_{13}$[51] and $LiZn_2(BH_4)_5$;[50] the former also showed $Al(BH_4)_3$ desorption and no trace of alane formation. In the case of $K[Al(BH_4)_4]$, we did not observe the fragments of $Al(BH_4)_3$ in the TGA-MS curve (Figure 6); however, the presence of 42 and 43, 56 and 57 amu likely belonging to $Al(BH_4)^+$ and $Al(BH_4)_2^+$ can be recognized in the logarithmic plot of the second TGA-MS experiment (Figure S7). Therefore, the decomposition by the reaction 3 can be affirmed with the maximum intensity of H_2^+ ion current at 160 °C.

This decomposition reaction pathway is different from the one for Li−Al borohydride, $Al_3Li_4(BH_4)_{13}$, desorbing $Al(BH_4)_3$ under vacuum,[51] and shows similarities with alkali metal−yttrium borohydrides, $M[Y(BH_4)_4]$, decomposing to hydrogen and nonvolatile amorphous MYB_4H_n (M = Li, Na, Rb, Cs and n = 4, 3, 3, 2, respectively) products.[52] Our manipulations with $K[Al(BH_4)_4]$ on air show its relatively good stability and non-explosive character, which is typical even for the smallest amounts of $Al(BH_4)_3$ vapors. No visible segregation of $Al(BH_4)_3$ from $K[Al(BH_4)_4]$ upon heating does not exclude that it stays in equilibrium with the starting compounds at temperatures close to ambient, forming a small partial pressure of aluminum borohydride. However, for potential applications in hydrogen storage it is important that this plausible reaction is not observed at elevated temperatures. This prompts further studies on reactive hydride composites capable of suppressing diborane release, and makes $K[Al(BH_4)_4]$ a good candidate for a conversion of aluminum borohydride in a more stable form, to be used for example in reactive hydride composites.[53]

Assessment of Rehydrogenation by *in Situ* Synchrotron X-ray Powder Diffraction. The sample with ≈84 wt % of $K[Al(BH_4)_4]$ was decomposed by heating up to 210 °C under 1 bar of H_2, using a single crystal sapphire cell shown in Figure 7a. It is the first system with $[Al(BH_4)_4]^-$ anion, characterized for reversibility by this method. Its thermal decomposition behavior reproduces the one under argon (compare Figures 7b and 1b). The decomposed material was loaded with 100 bar of H_2 at 50 °C, but no changes were observed by diffraction during the first 70 min (Figure 1c). The sample was heated rapidly to 320 °C and slowly cooled to the room temperature under 100 bar of hydrogen. We did not observe neither significant changes of intensities from KBH_4 of decomposed sample nor a formation of the starting $K[Al(BH_4)_4]$ (Figure 1d). Nonreversible character of $K[Al(BH_4)_4]$ decomposition is consistent with evolution of other gaseous species than hydrogen, such as gaseous B_2H_6 (see eq 3). Therefore, this composition alone is not suitable for direct rehydrogenation; its high hydrogen content allows for development of potentially reversible reactive hydride composites.[53]

Conclusions and Perspective. By direct interaction of potassium and aluminum borohydrides at room temperature, a complex borohydride, $K[Al(BH_4)_4]$, was obtained. According to the synchrotron X-ray powder diffraction study as well as vibrational spectroscopy, it contains distorted tetrahedral $[Al(BH_4)_4]^-$ anions, where the borohydride group is coordinated to aluminum via an edge. This is the first aluminum-based borohydride complex not stabilized by halide anions or by bulky organic cations. $K[Al(BH_4)_4]$ is not isostructural to bimetallic chlorides, where much more regular tetrahedral $AlCl_4^-$ anions are present. Instead, the complex borohydride is isomorphous to $TbAsO_4$ and reveals an anion $[Al(BH_4)_4]^-$ located in the bicapped trigonal prismatic cage K_8. Neglecting four longer $K\cdots BH_4$ distances, the structure can be also viewed as a framework built of two interpenetrated *dia*-type nets.

In situ X-ray powder diffraction, TGA, DSC, and TGA-MS data consistently show a single step of decomposition at ~160 °C, with an evolution of hydrogen with some amount of diborane. Aluminum borohydride is not released in substantial amounts; however, some crystalline KBH_4 forms upon decomposition. This contrasts with the decomposition of chloride-containing Li−Al borohydride, producing $Al(BH_4)_3$. The higher decomposition temperature of $K[Al(BH_4)_4]$ compared to the chloride-substituted Li−Al (70 °C) and Na−Al (90 °C) borohydrides suggests that the larger alkali metal cations (weaker Pearson acids) stabilize the weak Pearson base, $[Al(BH_4)_4]^-$. The hypothetic alkali earth aluminum borohydrides, such as $M[Al(BH_4)_4]_2$, are therefore expected to be unstable. On the contrary, the heavier alkali metal aluminum borohydrides, such as the title compound, are good candidates for storage of aluminum borohydride in a more stable form. This prompts further studies on reactive hydride composites,

dx.doi.org/10.1021/jp409217x | J. Phys. Chem. C 2014, 118, 145−153

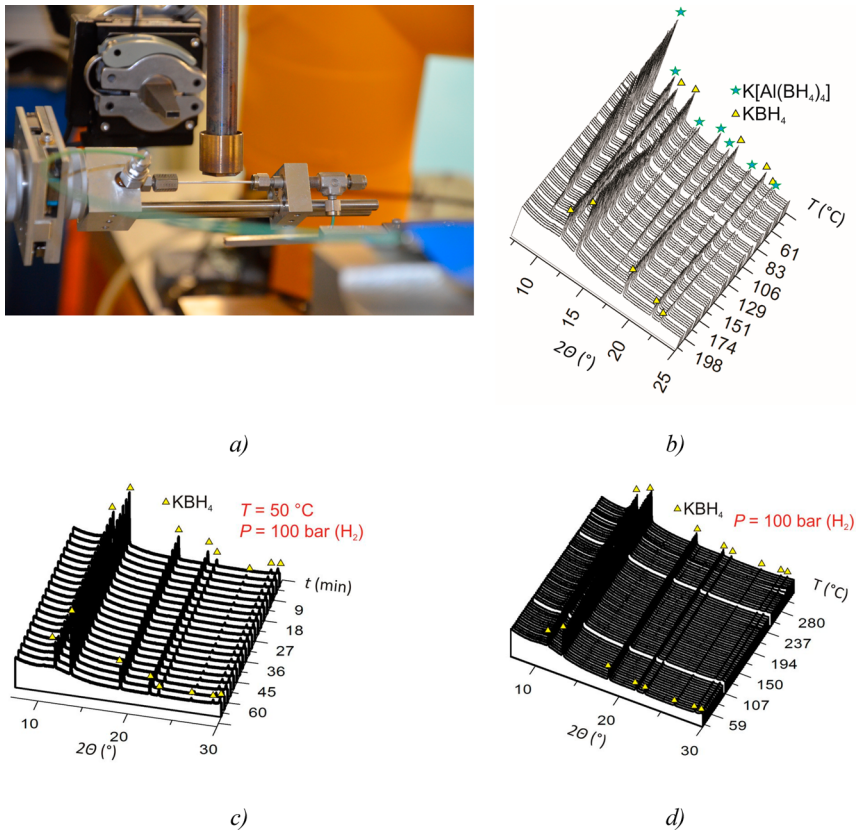

Figure 7. (a) Sapphire capillary filled with the sample and connected to the gas dosing system in the *in situ* synchrotron X-ray powder diffraction experiment. (b) Temperature evolution of powder diffraction patterns for $K[Al(BH_4)_4]/KBH_4$ mixture from 30 to 210 °C under 1 bar of H_2, resulting in the complete decomposition of $K[Al(BH_4)_4]$, λ = 0.775 045 Å, Material Science beamline at SLS. (c) Rehydrogenation of the decomposed $K[Al(BH_4)_4]/KBH_4$ mixture at 50 °C and 100 bar of H_2 for 70 min. (d) Rehydrogenation of the decomposed $K[Al(BH_4)_4]/KBH_4$ mixture at 100 bar of H_2 starting from 320 °C upon 10 °C/min cooling to room temperature.

such as $K[Al(BH_4)_4]$ plus a binary metal hydride, potentially capable to suppress diborane release.

After initial submission of our work, an independent study by Knight et al. was published,[54] reporting the crystal structure of $K[Al(BH_4)_4]$ in a noncentrosymmetric space group *Fdd*2. They did solid-state NMR and volumetric studies, which complement well our MS study of the decomposition and the assessment of rehydrogenation via *in situ* diffraction. Knight et al. report higher TGA mass loss on the decomposition, attributing it to a release of $Al(BH_4)_3$.

■ ASSOCIATED CONTENT

Supporting Information

Supplementary XRD data, Rietveld refinements, Raman spectra, temperature evolution of diffraction intensities, MS data, and a CIF file. This material is available free of charge via the Internet at http://pubs.acs.org.

■ AUTHOR INFORMATION

Corresponding Author

*Fax +32 10 47 27 07, e-mail yaroslav.filinchuk@uclouvain.be (Y.F.).

Notes

The authors declare no competing financial interest.

■ ACKNOWLEDGMENTS

This work was supported by the Académie Universitaire Louvain (AUL), Belgium, under Grant ADi/DB/1058.2011, by the Fonds de la Recherche Scientifique (FNRS), Belgium, under Grant 1.5169.12, and by the Swiss National Science Foundation. We are grateful to the Swiss−Norwegian Beamlines at the ESRF and the Materials Science Beamline at SLS for beamtime allocation and support. The research leading to these results has received funding from the European Community's Seventh Framework Programme (FP7/2007-2013) under grant agreement n.°312284 (CALIPSO). We thank J.-F. Statsyns for his help with TGA-MS measurements.

■ REFERENCES

(1) Orimo, S.; Nakamori, Y.; Eliseo, J. R.; Züttel, A.; Jensen, C. M. Complex Hydrides for Hydrogen Storage. *Chem. Rev.* **2007**, *107*, 4111−4132.

(2) Klebanoff, L. E.; Keller, J. O. 5 Years of Hydrogen Storage Research in the U.S. DOE Metal Hydride Center of Excellence (MHCoE). *Int. J. Hydrogen Energy* **2013**, *38*, 4533−4576.

(3) Züttel, A.; Rentsch, S.; Fischerb, P.; Wengera, P.; Sudana, P.; Maurona, Ph.; Emmenegger, Ch. Hydrogen Storage Properties of $LiBH_4$. *J. Alloys Compd.* **2003**, *356*−*357*, 515−520.

(4) Chłopek, K.; Frommen, C.; Lèon, A.; Zabara, O.; Fichtner, M. Synthesis and Properties of Magnesium Tetrahydroborate, $Mg(BH_4)_2$. *J. Mater. Chem.* **2007**, *17*, 3496−3503.

(5) Schrauzer, G. N. Uber ein Periodensystem der Metallboranate. *Naturwissenschaften* **1955**, *42*, 438.

(6) Nakamori, Y.; Miwa, K.; Ninomiya, A.; Li, H.; Ohba, N.; Towata, S.; Züttel, A.; Orimo, S. Correlation Between Thermodynamical Stabilities of Metal Borohydrides and Cation Electronegativities: First Principles Calculations and Experiments. *Phys. Rev. B* **2006**, *74*, 45126.

(7) Grochala, W.; Edwards, P. P. Thermal Decomposition of the Non-Interstitial Hydrides for the Storage and Production of Hydrogen. *Chem. Rev.* **2004**, *104*, 1283−1315.
(8) Lindemann, I.; Ferrer, R. D.; Dunsch, L.; Filinchuk, Y.; Černý, R.; Hagemann, H.; D'Anna, V.; Daku, L. M. L.; Schultz, L.; Gutfleisch, O. $Al_3Li_4(BH_4)_{13}$: a Complex Double-Cation Borohydride with a New Structure. *Chem.—Eur. J.* **2010**, *16*, 8707−8712.
(9) Lindemann, I.; Ferrer, R. D.; Dunsch, L.; Černý, R.; Hagemann, H.; D'Anna, V.; Filinchuk, Y.; Schultz, L.; Gutfleisch, O. Novel Sodium Aluminum Borohydride Containing the Complex Anion $[Al(BH_4,Cl)_4]^-$. *Faraday Discuss.* **2011**, *151*, 231−242.
(10) Ravnsbæk, D. B.; Filinchuk, Y.; Cerenius, Y.; Jakobsen, H. J.; Besenbacher, F.; Skibsted, J.; Jensen, T. R. *Angew. Chem., Int. Ed.* **2009**, *48*, 6659−6663.
(11) Ravnsbæk, D.; Sørensen, L. H.; Filinchuk, Y.; Besenbacher, F.; Jensen, T. R. A Series of Mixed-Metal Borohydrides. *Angew. Chem., Int. Ed.* **2012**, *51*, 3582−3586.
(12) Friedrichs, O.; Remhof, A.; Borgschulte, A.; Buchter, F.; Oriomo, S. I.; Züttel, A. Breaking the Passivation−the Road to a Solvent Free Borohydride Synthesis. *Phys. Chem. Chem. Phys.* **2010**, *12*, 10919−10922.
(13) Kim, K. C.; Hwang, S.-J.; Bowman, R. C., Jr.; Reiter, J. W.; Zan, J. A.; Kulleck, J. G.; Kabbour, H.; Majzoub, E. H.; Ozolins, V. $LiSc(BH_4)_4$ as a Hydrogen Storage Material: Multinuclear High-Resolution NMR and First-Principals Density Functional Theory Studies. *J. Phys. Chem. C* **2009**, *113*, 9956−9968.
(14) Černý, R.; Severa, G.; Ravnsbæk, D. B.; Filinchuk, Y.; D'Anna, V.; Hagemann, H.; Haase, D.; Jensen, C. M.; Jensen, T. R. $NaSc(BH_4)_4$: A Novel Scandium-Based Borohydride. *J. Phys. Chem. C* **2010**, *114*, 1357−1364.
(15) Černý, R.; Severa, G.; Ravnsbæk, D. B.; Filinchuk, Y.; D'Anna, V.; Hagemann, H.; Haase, D.; Skibsted, J.; Jensen, C. M.; Jensen, T. R. Structure and Characterization of $KSc(BH_4)_4$. *J. Phys. Chem. C* **2010**, *114*, 19540−19549.
(16) Jaroń, T.; Grochala, W. Probing Lewis Acidity of $Y(BH_4)_3$ via Its Reactions with MBH_4 (M = Li, Na, K, $N(Me)_4$). *Dalton Trans.* **2011**, *40*, 12808−12817.
(17) Huot, J.; Ravnsbæk, D. B.; Zhang, J.; Cuevas, F.; Latroche, M.; Jensen, T. R. Mechanochemical Synthesis of Hydrogen Storage Materials. *Prog. Mater. Sci.* **2013**, *58*, 30−75.
(18) Hagemann, H.; Černý, R. Synthetic Approaches to Inorganic Borohydrides. *Dalton Trans.* **2010**, *39*, 6006−6012.
(19) Ravnsbæk, D. B.; Sørensen, L. H.; Filinchuk, Y.; Reed, D.; Book, D.; Jacobsen, H. J.; Besenbacher, F.; Skibsted, J.; Jensen, T. R. Mixed-Anion and Mixed-Cation Borohydride $KZn(BH_4)Cl_2$: Synthesis, Structure and Thermal Decomposition. *Eur. J. Inorg. Chem.* **2010**, 1608−1612.
(20) Schlesinger, H. I.; Sanderson, R. T.; Burg, A. B. Metallo Borohydrides. I. Aluminum Borohydride. *J. Am. Chem. Soc.* **1940**, *62*, 3421−3425.
(21) Semenenko, K. N.; Kravchenko, O. V. Complex Compounds of Aluminium Tetrahydroborate with Potassium Chloride and Potassium Tetrahydroborate. *Russ. J. Inorg. Chem.* **1972**, *17*, 1084−1086.
(22) Schlesinger, H. I.; Brown, H. C.; Hyde, E. K. Preparation of Other Borohydrides by Metathetical Reactions Utilizing the Alkali Metal Borohydrides. *J. Am. Chem. Soc.* **1953**, *75*, 209−213.
(23) Mairesse, G.; Barbier, P.; Wignacourt, J.-P. Potassium Tetrachloroaluminate. *Acta Crystallogr.* **1978**, *B34*, 1328−1330.
(24) Hammersley, A. P.; Svensson, S. O.; Hanfland, M.; Fitch, A. N.; Häusermann, D. Two-Dimensional Detector Software: From Real Detector to Idealized Image or Two-Theta Scan. *High Pressure Res.* **1996**, *14*, 235−248.
(25) Willmott, P. R.; Meister, D.; Leake, S. J.; Lange, M.; Bergamaschi, A.; Böge, M.; Calvi, M.; Cancellieri, C.; Casati, N.; Cervellino, A.; et al. The Materials Science beamline upgrade at the Swiss Light Source. *Synchrotron Radiat.* **2013**, *20*, 667−682.
(26) Jensen, T. R.; Nielsen, T. K.; Filinchuk, Y.; Jørgensen, J.-E.; Cerenius, Y.; Gray, E. M.; Webb, C. J. Versatile *In Situ* Powder X-Ray Diffraction Cells for Solid-Gas Investigations. *J. Appl. Crystallogr.* **2010**, *43*, 1456−1463.
(27) Favre-Nicolin, V.; Černý, R. FOX, 'Free Objects for Crystallography': a Modular Approach to *Ab Initio* Structure Determination from Powder Diffraction. *J. Appl. Crystallogr.* **2002**, *35*, 734−743.
(28) Rodriguez-Carvajal, J. Recent Advances in Magnetic Structure Determination by Neutron Powder Diffraction. *J. Physica B* **1993**, *192*, 55−69.
(29) Spek, A. L. PLATON, University of Utrecht, The Netherlands, 2006.
(30) Soulié, J.-P.; Renaudin, G.; Černý, R.; Yvon, K. Lithium Boro-Hydride $LiBH_4$ I. Crystal Structure. *J. Alloys Compd.* **2002**, *346*, 200−205.
(31) Filinchuk, Y.; Chernyshov, D.; Dmitriev, V. Light Metal Borohydrides: Crystal Structures and Beyond. *Z. Kristallogr.* **2008**, *223*, 649−659.
(32) Nickels, E. A.; Jones, M. O.; David, W. I .F.; Johnson, S. R.; Lowton, R. L.; Sommariva, M.; Edwards, P. P. Tuning the Decomposition Temperature in Complex Hydrides: Synthesis of Mixed Alkali-Metal Borohydride. *Angew. Chem., Int. Ed.* **2008**, *47*, 2817−2819.
(33) Kim, K. C.; Sholl, D. S. Crystal Structures and Thermodynamic Investigations of $LiK(BH_4)_2$, KBH_4 and $NaBH_4$ from First Principles Calculations. *J. Phys. Chem. C* **2010**, *114*, 678−686.
(34) Dou, D.; Liu, J.; Krause Bauer, J. A.; Jordan, G. T., IV; Shore, S. G. Synthesis and Structure of Triphenylmethylphosphonium Tetrakis-(tetrahydroborato)aluminate, $[Ph_3MeP][Al(BH_4)_4]$ an Example of Eight-Coordinate Aluminum(III). *Inorg. Chem.* **1994**, *33*, 5443−5447.
(35) Schäfer, W.; Will, G.; Müller-Vogt, G. Refinement of the Crystal Structure of Terbium Arsenate $TbAsO_4$ at 77 and 5 K by Profile Analysis from Neutron Diffraction Powder Data. *Acta Crystallogr.* **1979**, *B35*, 588−592.
(36) Filinchuk, Y.; Černý, R.; Hagemann, H. Insight into $Mg(BH_4)_2$ with Synchrotron X-ray Diffraction: Structure Revision, Crystal Chemistry and Anomalous Thermal Expansion. *Chem. Mater.* **2009**, *21*, 925−933.
(37) Filinchuk, Y.; Richter, B.; Jensen, T. R.; Dmitriev, V.; Chernyshov, D.; Hagemann, H. Porous and Dense Magnesium Borohydride Frameworks: Synthesis, Stability, and Reversible Absorption of Guest Species. *Angew. Chem., Int. Ed.* **2011**, *50*, 11162−11166.
(38) Aldridge, S.; Blake, A. J.; Downs, A. J.; Gould, R. O.; Parsons, S.; Pulham, C. R. Some Tetrahydroborate Derivatives of Aluminum: Crystal Structures of Dimethylaluminium Tetrahydroborate and the α and β Phases of Aluminum Tris(tetrahydroborate) at Low Temperature. *J. Chem. Soc., Dalton Trans.* **1997**, 1007−1012.
(39) Almenningen, A.; Gundersen, G.; Haaland, A. On the Molecular Structure of Aluminum Borohydride, $Al(BH_4)_3$. *Acta Chem. Scand.* **1968**, *22*, 328−334.
(40) Krebs, B.; Greiwing, H.; Brendel, C. J.; Taulelle, F.; Gaune-Escard, M.; Berg, R. W. Crystallographic and Aluminum-27 NMR Study on Premelting Phenomena in Crystals of Sodium Tetrachloroaluminate. *Inorg. Chem.* **1991**, *30*, 981−988.
(41) Schouwink, P.; D'Anna, V.; Brix Ley, M.; Lawson Daku, L. M.; Richter, B.; Jensen, T. R.; Hagemann, H. Černý, R. Bimetallic Borohydrides in the System $M(BH_4)$-KBH_4 (M = Mg, Mn): On the Structural Diversity. *J. Phys. Chem. C* **2012**, *116*, 10829−10840.
(42) Rude, L. H.; Nielsen, T. K.; Ravnsbæk, D. B.; Bösenberg, U.; Ley, M. B.; Richter, B.; Arnbjerg, L. M.; Dornheim, M.; Filinchuk, Y.; Besenbacher, F.; et al. Tailoring Properties of Borohydrides for Hydrogen Storage: A Review. *Phys. Status Solidi A* **2011**, *208*, 1754−1773.
(43) Renaudin, G.; Gomes, S.; Hagemann, H.; Keller, L.; Yvon, K. Structural and Spectroscopic Studies on the Alkali Borohydrides MBH_4 (M = Na, K, Rb, Cs). *J. Alloys Compd.* **2004**, *375*, 98−106.
(44) Marks, T. J.; Kolb, J. R. Covalent Transition Metal, Lanthanide, and Actinide Tetrahydroborate Complexes. *Chem. Rev.* **1977**, *77*, 263−293.

(45) Makhaev, V. D. Structural and Dynamical Properties of Tetrahydroborate Complexes *Russ. Chem. Rev.* **2000**, *69*, 727−746.
(46) Coe, D. A.; Nibler, J. W. Infrared and Raman Spectra of Aluminum Borohydride, $Al(BH_4)_3$. *Spectrochim. Acta* **1973**, *29A*, 1789−1804.
(47) Dibeler, V. H.; Mohler, F. L. The Dissociation of Diborane by Electron Impact. *J. Am. Chem. Soc.* **1948**, *70*, 987−989.
(48) *NIST Chemistry WebBook, Mass Spectrum and Infrared Spectrum of Diborane, NIST Number 20*; National Institute of Standards and Technology: Gaithersburg, MD, 2005.
(49) Winkler, A.; Resch, Ch.; Redulic, K. D. Aluminum Hydride Desorption from Hydrogen Covered Aluminum Single Crystal Surfaces. *J. Chem. Phys.* **1991**, *95*, 7682−7688.
(50) Borgshulte, A.; Callini, E.; Probst, B.; Jain, A.; Kato, S.; Friedrichs, O.; Remhof, A.; Bielmann, M.; Ramirez-Cuesta, A. J.; Züttel, A. Impurity Gas Analysis of the Decomposition of Complex Hydrides. *J. Phys. Chem. C* **2011**, *115*, 17220−17226.
(51) Lindemann, I.; Borgschulte, A.; Callini, E.; Züttel, A.; Schultz, L.; Gutfleisch, O. Insight into the Decomposition Pathway of the Complex Hydride $Al_3Li_4(BH_4)_{13}$. *Int. J. Hydrogen Energy* **2013**, *38*, 2790−2795.
(52) Jaroń, T.; Wegner, W.; Grochala, W. $M[Y(BH_4)_4]$ and $M_2Li[Y(BH_4)_{6-x}Cl_x]$ (M = Rb, Cs): New Borohydride Derivatives of Yttrium and Their Hydrogen Storage Properties. *Dalton Trans.* **2013**, *42*, 6886−6893.
(53) Alapati, S. V.; Johnson, J. K.; Sholl, D. S. Large-scale Screening of Metal Hydride Mixtures for High-Capacity Hydrogen Storage from First-Principles Calculations. *J. Phys. Chem. C* **2008**, *112*, 5258−5262.
(54) Knight, D. A.; Zidan, R.; Lascola, R.; Mohtadi, R.; Ling, C.; Sivasubramanian, P.; Kaduk, J. A.; Hwang, S.-J.; Samanta, D.; Jena, P. Synthesis, Characterization, and Atomistic Modeling of Stabilized Highly Pyrophoric $Al(BH_4)_3$ via the Formation of the Hypersalt $K[Al(BH_4)_4]$. *J. Phys. Chem. C* **2013**, *117*, 19905−19915.